Available online at www.sciencedirect.com
ScienceDirect
Carbohydrate Polymers 67 (2007) 245–255
Carbohydrate Polymers
www.elsevier.com/locate/carbpol

Blue agave fiber esterification for the reinforcement of thermoplastic composites

E. Tronc [a], C.A. Hernández-Escobar [b], R. Ibarra-Gómez [b], A. Estrada-Monje [b], J. Navarrete-Bolaños [c], E.A. Zaragoza-Contreras [b,*]

[a] *Laboratoire de Chimie Agro-Industrialle, UMR INRA, Ecole Nationale Supérieure de Chimie de Toulouse, INP Toulouse, 118 route de Narbonne, 31077 Toulousse Cedex 04, France*
[b] *Centro de Investigación en Materiales Avanzados, S.C., Miguel de Cervantes No. 120, Complejo Industrial Chihuahua, CP 31109, Chihuahua Chih, México*
[c] *Instituto Mexicano del Petróleo, Eje Central Lázaro Cárdenas No. 152, Col. Sn. Bartolo Atepehuacan, CP 07730, México, DF, México*

Received 10 September 2004; received in revised form 26 April 2006; accepted 30 May 2006
Available online 23 August 2006

Abstract

Blue agave fiber esterification and its use in thermoplastic composite reinforcement was the purpose of this research. Spectroscopic techniques indicated the occurrence of the esterification reaction, since signals for carbonyl groups were found through FT-IR (1750 cm^{-1}) and ^{13}C-CPMAS-NMR (172 ppm). Mechanical properties characterization showed that superficial modification was successfully achieved, since a change in the elastic modulus and improved impact resistance were observed when the modified fiber was used. In addition, electron microscopy studies indicated that the modified fiber produced an enhancement in fiber/HDPE interfacial interaction, since less fiber sliding evidence was observed on the composite surface. The Cox–Merz rule was used as an alternative tool in order to study composites rheometry along an expanded range of shear rate in the power law region.

Keywords: Lignocellulosic; Blue agave fiber; Esterification; Thermoplastic composite; Rheology

1. Introduction

Lignocellulosics are biodegradable materials that nature recycles through biological, thermal, chemical and photochemical processes. Theses materials are hygroscopic by nature, since they are designed to perform in a wet environment. The chemical constitution of lignocellulosics varies from specie to specie but cellulose, hemicelluloses and lignin are the common constituents. Annually large amounts of lignocellulosics are produced as wastes, where wood and its derivatives constitute around 40% of the residual solid wastes from residential, commercial, industrial and institutional sources. Since lignocellulosic fibers can improve the toughness and strength of plastics, the production of thermoplastic composites is becoming important in applications for recovering and recycling these materials. However, as mentioned above, the hydrophilic nature of lignocellulosics difficult their interaction with most thermoplastic polymers and the resulting composites present poor mechanical properties. In order to improve the interfacial interaction lignocellulosic/thermoplastic, the modification of one of them should be achieved. In general, it is convenient to modify the fiber through physical or chemical methods. Physical methods include: corona or plasma treatments and mercerization, where fiber surface is modified by influencing its mechanical bonding with the polymeric matrix; whereas chemical methods consist in the reaction of some groups of the fiber with a proper reactive

* Corresponding author. Tel.: +52 614 439 4811; fax: +52 614 439 4811.
E-mail address: armando.zaragoza@cimav.edu.mx (E.A. Zaragoza-Contreras).

0144-8617/$ - see front matter © 2006 Elsevier Ltd. All rights reserved.
doi:10.1016/j.carbpol.2006.05.027

compound in order to form covalent bonds. The new component acts as an interface between both the fiber and the thermoplastic matrix, thus improving composite performance as a result of a better interfacial interaction (Bledzki & Gassan, 1999).

There are two main techniques for carrying out lignocellulosics chemical modification; the first technique consists of grafting polymeric chains on the fiber surface by forming free radicals using a redox-initiator and subsequently, propagate polymeric chains (Gupta & Sahoo, 2001; Gürdağ, Yaşar, & Gürkaynak, 1997; Gürdağ, Güclü, & Özgümüş, 2001; Huang, Zhao, Zheng, He, & Gao, 1992; Mohanty, Mubarak, & Hinrichsen, 2000; Román-Aguirre, Márquez-Lucero, & Zaragoza-Contreras, 2004). The second method includes the reaction of the cellulose hydroxyl groups (OH) with certain kinds of reagents such as silanes (Coutinho, Costa, Carvalho, Gorelova, & Claudio de Santa Maria, 1998; Redondo, Radovanovic, Goncalves, & Yoshida, 2002; Rong, Zhang, Liu, Yang, & Zeng, 2001), acyl halogenures (Chuavelon et al., 1999; Nair, Thomas, & Groeninckx, 2001; Sun, Fan, Tomkinson, Geng, & Liu, 2001; Thiebaud & Borredon, 1995; Thiebaud, Borredon, Baziard, & Senocq, 1997), isocianates (Ellis & O'Dell, 1999; Joseph, Rabello, Mattoso, Joseph, & Thomas, 2002; Vázquez, Domínguez, & Kenny, 1999), carboxylic acids (Rong et al., 2001; Sun, Sun, & Sun, 2002) or anhydrides (Rowell et al., 1994; Sun et al., 2002; Vaca-García & Borredon, 1999; Vaca-García, Thiebaud, Borredon, & Gozzelino, 1998). Commonly, these reagents have reactionable functional groups where a polymer chain can be propagated or grafted (Joseph et al., 2002). The effect of lignocellulosics chemical modification is the reduction of hydrophilicity (if the new group lignocellulosic-modifier is hydrophobic), which in first instance should solve the problem related to polarity differences between the fiber and the thermoplastic.

As mentioned above, the chemical modification produces changes on the fiber hydrophilicity, which should improve the interfacial interaction fiber/thermoplastic and the composite mechanical performance. The present research was aimed to study the chemical modification of a lignocellulosic fiber; such modification consisted in the esterification reaction between the cellulosic fraction of the fiber and a nonsymmetric anhydride (in non-aqueous media). It is worthy to mention that solid ^{13}C NMR was used as a basic tool in order to obtain strong evidence about the modified fiber structure. The fiber used was an agro-industrial waste derived from Weber blue agave fiber (*agave tequilana weber blue variety or agave palmaris*) which grows in Western Mexico (Jalisco) and through its fermentation tequila has been produced for long time. With tequila massive industrialization, large amounts of fiber are produced yearly as byproduct, and together with many other similar materials, its accumulation and disposal has become a critical environmental problem (Iñiguez-Covarrubias, Lange, & Rowell, 2001). The study was complemented with the evaluation of mechanical properties of fiber/polyethylene (HDPE) composites and the obtention of viscosity curves applying the Cox–Merz rule.

2. Experimental

2.1. Chemicals

In order to achieve fiber chemical modification the following reagents were used: acetic anhydride (J.T. Baker), octanoic acid (Aldrich Co.) and acetone (Fisher), all of them used as received. The used water was tridistillated quality. Prior to modification the fiber was washed with warm water in order to eliminate dust and sugar remains from the fermentation process. Afterwards, the fiber was dried in an air convection oven at 110 °C for 24 h. Finally, the fiber was milled in a rotatory mill. The fiber aspect radio (length/diameter, relationship), determined by measuring around 800 fibers (optic microscopy and image analysis), was 13.24. It is important to mention that fiber population was conformed by two groups of size; the first of finely milled fiber [powder (40% weight) = 0.007 to 1.0 mm] and the second, of larger fiber [long fiber (60% weight) = 1.001 to 10.0 mm]. High-density polyethylene (HDPE) from Chevron (Marflex Hi-D94312; MI = 12; $\rho = 0.943\ g\ cm^{-3}$) was used as the composite matrix.

2.2. Esterification

The fiber modification was performed by using a similar system, acetic anhydride/octanoic acid, as reported in literature (Vaca-García et al., 1998). However, in the present work the fiber was not milled completely to powder but was kept to a much longer average size, in order to evaluate a broad distribution of fiber size. It has to be mentioned that the fiber for composite formulation was not selected in a particular size range but used as obtained form the mill. That was due to the fact that after milling the fiber, around 40% weight of it was obtained as powder and the rest as long fiber (60% weight), so for practical purposes and to use as much fiber as possible, it was decided to use it as a mixture, with the characteristics mentioned above.

The esterification reaction was carried out in a three-neck-round-bottomed flask of 1000 mL provided with mechanical agitation and a glass condenser. A typical experiment was performed as follows: 190 mL (2.0 eq) of acetic anhydride and 888 mL (5.6 eq) of octanoic acid were mechanically mixed (200 rpm) for 1.0 h at 90 °C. These compounds react to form a so-called mixed anhydride ($MAn = CH_3–OCOCO–(CH_2)_6–CH_3$). Next, the corresponding amount to 2.0 eq of fiber (108.0 g) was added to MAn. The reaction mixture was allowed to react for 3.0 h at 135 °C with mechanical agitation. After the reaction time the modified fiber was cleaned by extraction with acetone; the fiber was considered clean once any remain of MAn was not visible and any scent

of the mixture was not perceived. Finally, in order to evaporate the solvent the fiber was put into an air convection oven at 50 °C for 6 h.

2.3. Ester content

The ester content was calculated according to a reported method (Girerdeau et al., 2001) as follows: first, 1.0 g of modified fiber plus 40 mL of ethanol (95%) were loaded into a glass recipient and heated at 55 °C for 30 min. Next, 25 mL of a sodium hydroxide (NaOH) aqueous solution 0.5 N was added and let in agitation for 15 min more at 55 °C. The mixture was kept in repose for 3 days at room temperature. Afterwards, NaOH solution was fed in order to saponificate the formed ester groups. The saponification process consumed certain amount of NaOH, which was determined by titration with a hydrochloric acid (HCl) aqueous solution 0.5 N, using phenolphthalein as color indicator. A blank sample (unmodified fiber) was also treated through the same described method in order to have a reference for comparison. The difference in concentration of HCl solution used for titrating the blank sample and the modified sample determines the concentration of NaOH involved in the saponification of the ester groups (or the formed ones during esterification). The ester content (EC) was determined according to the following equation:

$$\mathrm{EC}(\%) = [(A - B) * N_{\mathrm{B}} - (C - D) * N_{\mathrm{A}}] * \frac{M}{10 * W}, \qquad (1)$$

where A and B are the volume (mL) of NaOH solution added to the modified sample and to the blank, respectively. C and D are the volume (mL) of HCl solution used to neutralize the modified sample and the blank, respectively. N_{A} and N_{B} are the normal concentration (N) of the HCl and NaOH, respectively. W is the weight of the sample and M the molar mass of the grafted acyl group.

2.4. Oil/water test

A qualitative *oil/water* test was performed in order to evaluate the new hydrophobic property of the modified fiber. Samples of 1.5 g of unmodified and modified fiber were loaded in separate recipients, where 50 mL of tap water were previously added. Afterwards, the fiber samples were allowed to hydrate for 5 min and 10 mL of mineral oil were added to every recipient. Finally, the mixture was thoroughly mixed and let in repose for 30 min.

2.5. Infrared spectroscopy (FT-IR)

Esterification product was characterized by infrared spectroscopy. The analyses were performed in a FT-IR Nicolett Series 2 Magna IR 750. Before running the spectra, the samples of modified and unmodified fiber were dried at 110 °C for 12 h. The samples were analyzed through the KBr tablet technique.

2.6. Solids ^{13}C NMR

Nuclear magnetic resonance (NMR) spectra were run using a Bruker 300 JCAMPDX-V1.0 spectrometer operating at 100 MHz for ^{13}C and 400 KHz for ^{1}H. Spectra acquisition was performed at 6 KHz using a zirconium oxide rotor of 4 mm. ^{13}C NMR spectra were performed in the cross-polarization mode with magic angle spin (CPMAS).

2.7. Thermal properties

To evaluate chemical modification effects on the fiber thermal properties, thermogravimetric analysis (TGA) and differential thermal analysis (DTA) were performed. Thermograms were run on a simultaneous TGA–DTA TA Instruments SDT 2960, under air atmosphere. The analyses were carried out at a heating speed of 10 °C/min. Prior to analysis the samples were dried at 110 °C for 12 h.

2.8. X-ray diffraction

X-ray measurements were run on a Philips X-Pert diffractometer at 40 KV and 30 mA, under the following conditions: start angle $(2\Theta) = 5°$, end angle $(2\Theta) = 80°$, step size $(2\Theta) = 0.1°$, time/step (s) = 5 and scanning time (h:min:s) = 1:0:0.

2.9. Mechanical properties

Fiber/HDPE composites, with different contents of modified or unmodified fiber, were prepared in order to evaluate the effect of both modification and fiber content on the composites mechanical properties. Samples were prepared according to ASTM-D 256 and ASTM-D 790 procedures. The samples were prepared as follow: first, a series of mixtures fiber/HDPE were prepared using a mixing chamber of 60 cm^3 (coupled to a Plasticorder C.W. Brabender) at 180 °C and 30 rpm. Second, plaques (15×15 cm and 2.0 mm wide) were prepared by compression molding at 10 metric tons and 200 °C. A CEAST model CCF-50 device was used to machine the probes. Third, composite impact resistance was determined by using an Izod analyzer with 12 cm and 0.245 g of length and pendulous mass, respectively. Fourth, Young module of samples was determined with an Instron series 4301 connected to a PC for data acquisition. Finally, samples were run using 5 kN cells at room temperature.

2.10. Scanning electron microscopy

The interfacial interaction fiber/HDPE was analyzed by scanning electron microscopy (SEM) in a SEM Jeol Model 5800 LV. Samples were prepared by frizzing the probes with liquid nitrogen and breaking them with the Izod

analyzer; before the analyses the composite samples were covered with gold in order to avoid static charge.

2.11. Rheology

Composite viscosity curves were performed with a Haake Rheostress 150 universal rheometer. Cone and plate geometry was used in both rotational and oscillatory modes at 160 °C. Fixed stress for frequency sweep in oscillatory motion was 10 Pa.

3. Results and discussion

3.1. Degree of substitution (esterification)

Before discussing esterification characterization, it has to be mentioned that lignocellulosics structure is constituted by several layers concentrically arranged and with different composition. Each fiber is formed by a series of microfibril aggregates into longer macrofibril helically wounded along the fiber axis and embedded into an amorphous lignin/hemicelluloses matrix (Rong et al., 2001). Considering lignocellulosics structure is important since in this research it was assumed that only the cellulosic fraction participate in the esterification reaction. The method used in this research comprises the reaction of a non-symmetric anhydride [MAn = CH_3–OCOCO–$(CH_2)_6$–CH_3] with the cellulose hydroxyl (OH) groups, where the octanoic acid reacts first with the acetic anhydride (co-reagent) in order to produce a more reactive specie (with OH groups of cellulose) than the fatty acid by itself (Vaca-García et al., 1998). Experimentation indicated that the esterification depended importantly on the fiber size (powder or long fiber). As can be seen in Table 1, the fraction of powder fiber presented ester content three times higher than the long ones. It is believed that in the case of the powder the diffusion of the reaction mixture (MAn) towards the richer cellulose regions was more efficient than in the case of the long fiber, where the amorphous phase lignin/hemicelluloses apparently restricted MAn diffusion towards cellulose. Therefore, and in accordance with these results, it is evident that the external layers in the long fiber structure are not appropriate enough for the esterification reaction.

3.2. Hydrophobicity

A performed water/oil test showed important differences between the modified (a) and the unmodified (b) fiber. Fig. 1 illustrates both mixtures; first, it was observed that once the oil was added, the modified fiber ascended immediately as the organic phase separated from the water. On the contrary, the unmodified sample tended gradually to settle on the recipients bottom, showing its preference for the polar phase. It was evident that surface nature of both fiber samples was quite different, thus the modified fiber showed clearly its new hydrophobic character, which was attributed to the low polarity of formed ester groups, in comparison to the cellulose hydroxyl groups (highly polar). According to this new feature, the hydrophobic fiber should present an improved compatibility with low polar thermoplastics, because of an expected enhanced superficial impregnation of the treated fiber with the matrix.

Table 1
Esterification content and substitution degree of blue agave fiber modified with the mixed anhydride

Fiber	Ester content (%)	Substitution degree
Long	13.57	0.34
Powder	34	1.17

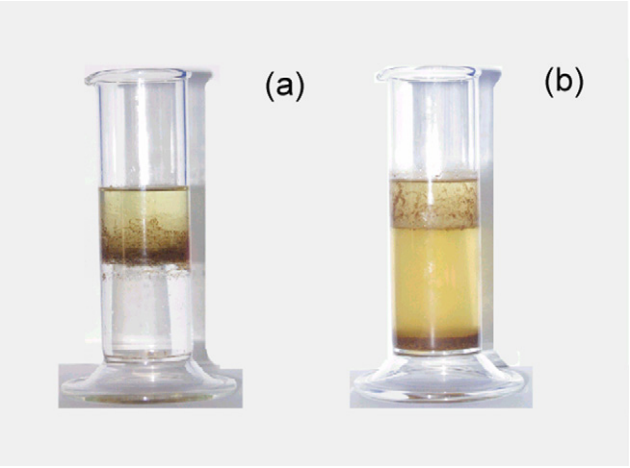

Fig. 1. Qualitative test of hydrophobicity—water/oil—for (a) modified and (b) unmodified fiber.

3.2.1. Infrared spectroscopy (FT-IR)

The changes suffered by the fiber as a consequence of the esterification reaction were followed by FT-IR spectroscopy. The spectra for both fibers, unmodified (a) and modified (b), are shown in Fig. 2. Similarly to all lignocellulosics, agave fiber presents the typical signals of a combination of cellulose and lignin. The spectrum (a) has a broad peak at 3429 cm^{-1} typical for hydroxyl groups of cellulose (O–H); it is also observed a small peak at 1734 cm^{-1} corresponding to the carbonyl groups (C=O) due to the presence of acetyl ester and carbonyl aldehyde groups on hemicelluloses and lignin, respectively (Hassan, Rowell, Fadl, Yacoub, & Christainsen, 2000, 2000; Matuana, Balatinecz, Sodhi, & Park, 2001); the peak at 1625 cm^{-1} apparently do not belongs to the fiber; however, its presence has been associated to absorbed water and is commonly observed on lignocellulosics spectra (Kontturi, Thüne, & Niemantsverdriet, 2003; Loría-Bastarrachea, Carrillo-Escalante, & Aguilar-Vega, 2002; Sun et al., 2001). The peaks at 2924 and 2846 cm^{-1}, due to vibrations of C–H (methyl groups), and those observed at 1070, 1040 and 900 cm^{-1}, due to the group C–O, are associated to the structure of the glucopyranose ring (repetitive unit of cellulose) (Kontturi et al., 2003). While, the spectrum (b) shows clearly an intense peak at 1750 cm^{-1} typical for C=O of ester groups that overlaps the one observed at 1734 cm^{-1}

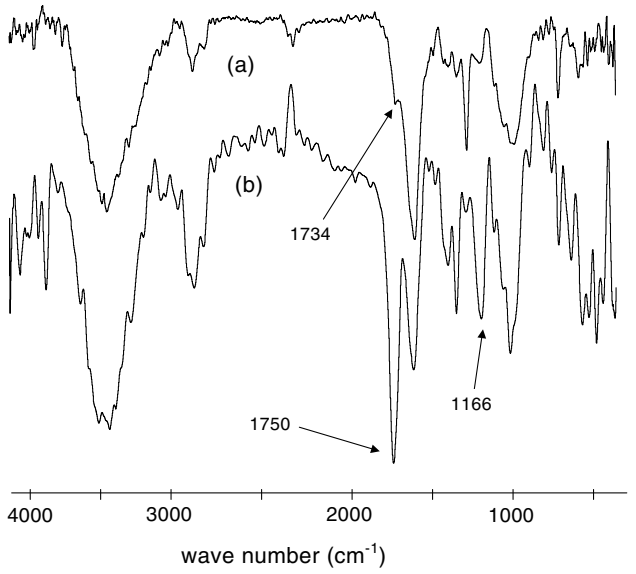

Fig. 2. Infrared spectra for unmodified (a) and modified (b) blue agave fiber.

in spectrum (a). Similarly, it is observed that the peak at 1160 cm^{-1} is now more intense than in spectrum (a). Comparable results have been found in literature for the esterification of bagasse fiber (Hassan et al., 2000, Hassan, Rowell, Fadl, Yacoub, & Christainsen, 2000) and cellulose (Jandura, Kokta, & Riedl, 2000) with fatty acids and hemicelluloses with acyl chlorides (Sun et al., 2001), and it was attributed to the formation of C–O–C of ester groups. The two mentioned signals and those at 2960, 2918 and 2867 cm^{-1} (all due to C–H of methylene groups) indicate the presence of alkyl chains and ester groups on the fiber produced by the reaction of the octanoic fraction of the mixed anhydride (MAn) with the cellulose.

3.2.2. Solid ^{13}C cross-polarization magic angle spinning NMR spectroscopy (^{13}C CPMAS NMR)

^{13}C CPMAS NMR is an appropriate technique to study fiber samples in its native state. Through ^{13}C CPMAS NMR it is possible to differentiate signals for crystalline or amorphous carbons in cellulose because of differences in magnetic environment due to changes in packing or in conformation. ^{13}C CPMAS NMR spectrum for the unmodified fiber is shown in Fig. 3. Before describing this figure, it has to be mentioned that the assignation of the different carbon signals was achieved according to literature (Atalla, Gast, Sindorf, Bartuska, & Maciel, 1980; Czimczik, Preston, Schmidt, Werner, & Schulze, 2002; Jandura et al., 2000; Sun et al., 2001). In one hand, Fig. 3 shows mainly the corresponding signals for the cellulose; however, signals for lignin are also observed even though spectrum noisiness. Thus, the peaks at 103.7 (C1), 88.2 (C4) and 64.8 ppm (C6) are reported to correspond to cellulose carbons in glucopyranose rings within crystalline packing. On the other hand, the peaks at 83 (C4′) and 63 ppm (C6′) correspond also to carbons in glucopyranose rings but within amorphous regions. Lignin is a quite complex amorphous macromolecule with coniferyl and cinapyl alcohols as the most common minimal units in its composition. Depending on the abundance of some of these alcohols the spectrum presents certain characteristics, as described for Czimczik et al. (2002). Letter L is preceding lignin carbons in order to differentiate them from those of cellulose. Thus, methoxy carbons of lignin ($–OCH_3$) are observed at 56 ppm, the signals for CL3 and CL5 (aromatic carbons) are observed at 153 ppm, a wide peak between 125 and 140 ppm and a another one, which should appear close to 110 ppm, which cannot be observed due to overlapping with the prominent peak at 103.7 ppm for C1 of cellulose, corresponds to CL1 and CL4. In the alkyl region (10–35 ppm), a series of peaks are observed, which are attributed to methyl and alkyl carbons of lignin. Two more signals are also observed, one at 22 ppm assigned as acetate carbons and a second one, between 165 and 177 ppm, which corresponds to carboxyl.

Fig. 4 shows the ^{13}C CPMAS NMR spectrum for the esterified fiber. Here, it is possible to observe between 50 and 106 ppm the corresponding signals for cellulose. However, in this figure lignin signals were not easy to distinguish, since they were overlapped for other more prominent ones; therefore, they were not included in the discussion. It is worthy to mention that the reaction MAn/cellulose has two possible results, (i) cell–O–CO–CH_3 or (ii) cell–O–CO–$(CH_2)_6$–CH_3. Substituents similarity makes difficult their individual characterization; however, the signals for specie (ii) can be assigned without any problem. The peak at 15 ppm corresponds to C14 and the signals between 20 and 33 ppm are typical for the methylene groups of the alkyl chain (C8 to C13). The corresponding signal to the ester groups (C7) appears at 172 ppm. This signal and other observed at 1749 cm^{-1} in the FT-IR spectrum (Fig. 2) are very important since they indicate the occurrence of the esterification reaction. At this point a second aspect has to be considered too, that the glucopyranose rings have three possible points for reacting with MAn, a, b and c (Fig. 3). According to this, some (or all) of the signals for C2, C3 or C6 should present some change as evidence of the reaction. In Fig. 4 it could be clearly observed that the peaks for C2 and C3 almost disappeared, as well as the one for C6′. In addition, it must be noted that a new peak appeared at 55 ppm which can be attributed to the formation of C6″ (cell–C6″–COO–) and the peak at 65 ppm has become both larger and sharper with respect to the observed for C6 in Fig. 3. This modification suggests the formation of C2′ and C3′ (cell—COO–) whose signals should appear at this position. Therefore, it is clear that the three points (a, b and c) have reacted with MAn confirming, again, the esterification reaction.

3.3. Thermal analysis

The evaluation of fiber thermal stability is an important aspect since this is a critical property for the thermoplastic

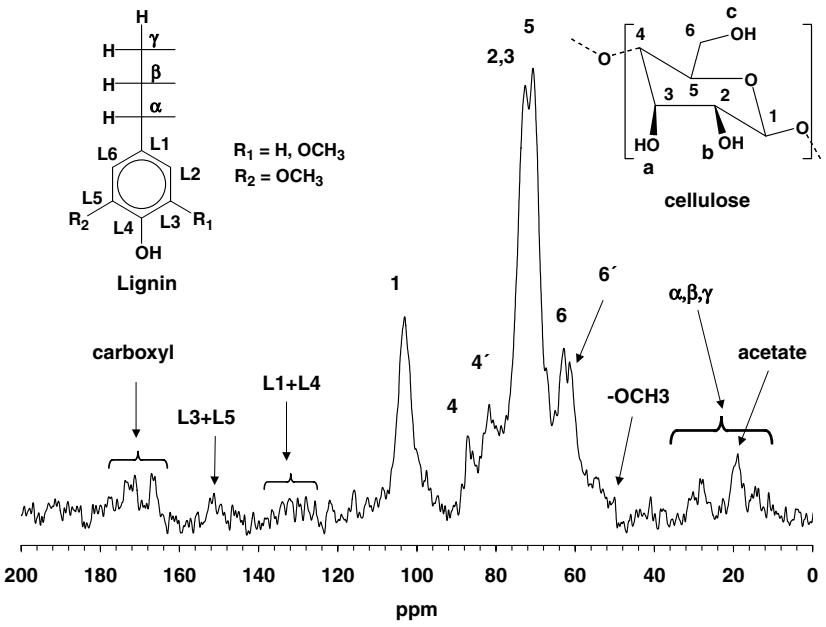

Fig. 3. CP/MAS ^{13}C NMR spectrum for blue agave fiber before modification.

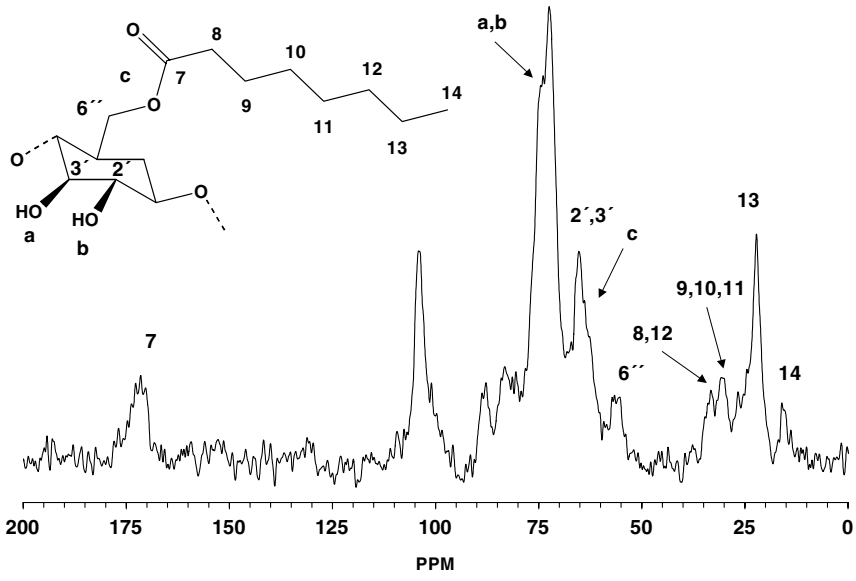

Fig. 4. CP/MAS ^{13}C NMR spectrum for blue agave fiber after esterification.

composite processing, considering the relatively low degradation temperature of lignocellulosics. The graphs of TGA for the modified (a) and the unmodified (b) fiber are shown in Fig. 5. It is observed that degradation temperature for the modified fiber starts at 290 °C, which is higher than the showed for the unmodified fiber (270 °C). Similar increments in thermal stability have been found in literature for other treatments (Ghosh & Ganguly, 1994; Rahman et al., 2000). In the present case, such increment could be associated to the formation of ester groups; however, this effect is not always produced by the esterification, as reported by Hassan et al. (2000, 2000) or Coutinho et al. (1998). DTA plots for both fiber samples are also included in Fig. 5. Here, two maximum values in degradation temperature are observed for each sample, the first at 350 °C, which corresponds to fiber degradation, and a second at 450 °C, typical for the oxidation of carbon compounds. DTA also showed a slight difference in fiber thermal stability, since the maximum decomposition temperature for the modified fibers (a) was 10 °C higher than the one for the unmodified fiber (b), being in agreement with TGA analysis.

3.4. X-ray diffraction

Crystallinity in lignocellulosics is a feature derived from cellulose structure which consists of polymeric glucopyranose chains helicoidally arranged and strongly linked by

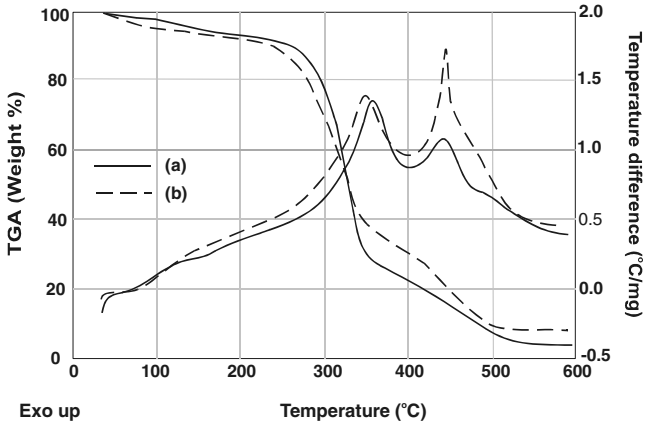

Fig. 5. TGA-DTA thermograms for (a) modified and (b) unmodified fiber.

hydrogen bonds. X-ray diffraction diagrams, for the modified and the unmodified agave fiber, are shown in Fig. 6. It can be observed in this figure that before modification (a) the fiber did not present exactly the typical crystalline pattern either for cellulose or lignocellulosics, since the peaks at $2\Theta = 15°$, 24.5° and 30.5° are not reported. The diffractogram for the modified fiber (c) presented, however, some differences, since the peaks mentioned above almost disappeared. In order to determine whether or not the modification caused the observed changes, a fiber sample was carefully washed with hot water and acetone, similarly as the treated fiber during the cleaning process. The spectrum of the unmodified clean fiber (b) showed, indeed, that the peaks in discussion were reduced importantly, indicating that the changes in those were not related to the fiber modification. It is believed that those signals were produced by some substance(s) which impregnated on the fiber during the fermentation process or byproducts confinement. If the mentioned peaks are not considered, it is possible to observe that the pattern for the unmodified clean fiber (b), in particular the peaks at $2\Theta = 14.9°$ and 16.5°, which are reported for cellulose, presented a decrement once the modification was performed (c). Similar observation has been reported as effect of the cellulose modification (Chuavelon et al., 1999; Jandura et al., 2000; Kim, Kuga, Wada, Okano, & Kondo, 2000; Rong et al., 2001) and can be explained considering that the formation of ester groups opens hydrogen bonds, turning crystalline cellulose into amorphous.

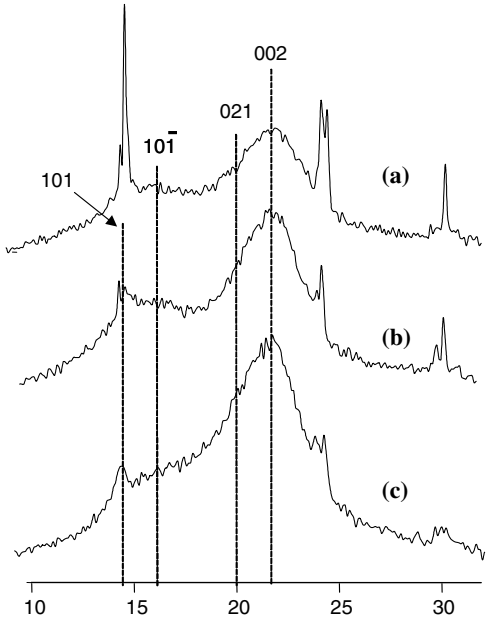

Fig. 6. X-ray diffraction diagrams for (a) fiber before esterification, (b) fiber after extraction with water and acetone and (b) esterified fiber.

3.5. Mechanical properties

Elasticity modulus (EM) for fiber/HDPE composites, at different fiber HDPE weight ratios, is shown in Fig. 7. In this test, the composites with modified or unmodified fiber were evaluated. It can be seen that EM increased progressively with the fiber content, as has been reported in other works (Coutinho, Costa, & Carvalho, 1997; Rana, Mandal, & Banerjee, 2000; Ray, Sarkar, Das, & Rana, 2002; Xu, Simonsen, & Rochefort, 2001). Such increment is a consequence of the incorporation of a rigid phase, with less energy dissipative effect, than the plastic matrix. However, it is noticeable that the modified fiber composites exhibit a lower modulus than the unmodified ones. In this sense, it is possible that the adhesion mechanism had conferred a ductile character to the fiber/matrix interface (Balasuriya, Ye, Mai, & Wu, 2002). This argument is supported by the impact strength (IS) behavior, Fig. 8, since IS for the modified fiber composites was predominantly higher for each fiber concentrations, even tough this property decreases, in general, with the fiber content. Again, it is suggested that the interface structure generated by the esterification promotes energy absorption, which is not present in the unmodified composites where fiber dewetting causes that the matrix/fiber interface defects, act as crack propagating

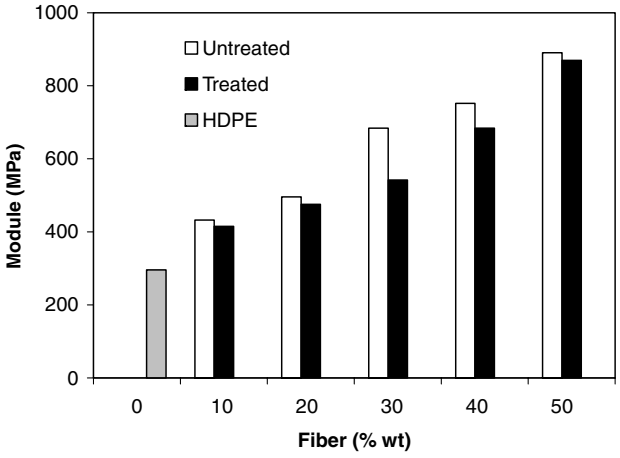

Fig. 7. Effect of fiber content on the modulus of fiber/HDPE composites using (white) unmodified fiber or (black) modified fiber.

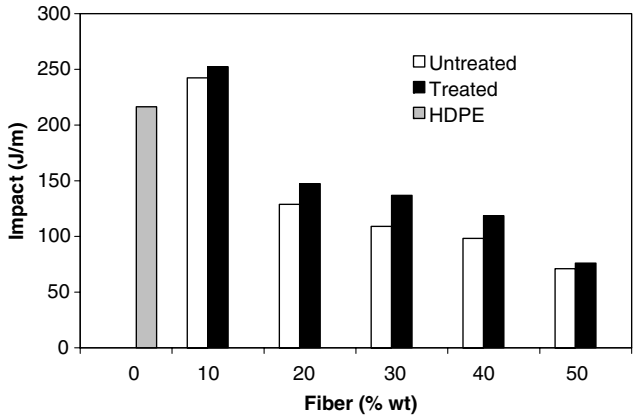

Fig. 8. Effect of fiber content on the Izod impact strength of fiber/HDPE composites using (a) unmodified or (b) modified fiber.

points (Nielsen & Landel, 1994). The apparently ductile character showed by the modified composite is related to the compatibilized interface nature (Balasuriya et al., 2002). According to that, the presence of large regions of eight-carbon chains, due to the graft of octyl radicals are expected.

The higher impact strength observed at 10% wt of fiber content, respect to the pure HDPE, could indicate a better fiber wetting, in virtue that at this concentration the fiber is more isolated than at higher concentrations, where the fiber agglomeration apparently promotes a weaker wetting. The dropping of the impact strength with the filler content could be associated to the presence of fiber powder, producing a wide distribution of aspect ratio. In these sense, it has been established that the fracture work for short fiber is proportional to the square of the fiber length (Simonsen, Jacobsen, & Rowell, 1998). Thus, the powder would represent points of weakness for crack propagation. Nevertheless, it has to be mentioned that the fiber was homogeneously used during composite preparation in order to avoid effects due to fiber size inhomogenity.

3.6. Microscopy

Fiber surface modification was achieved in order to enhance the interfacial interaction between the fiber (high polarity) and the thermoplastic matrix (low polarity), which should produce an improvement in the composite impact strength. Such improvement is related to an enhanced adhesion of the matrix over the fiber surface. Micrographs for the composite samples using unmodified (a) or modified (b) fiber, both at a rate of 50/50% wt of fiber to HDPE, are shown in Fig. 9. In micrograph (a) a lot of cavities, where fibers were supposed to be imbedded, are observed. It is assumed that due to the impact, during sample preparation, the fibers slipped away from the matrix because of a deficient adhesion. Whereas on micrograph (b), even though evidence of fiber sliding can be observed, the fibers were better attached to the matrix, since fractions of fractured fibers are present inside some

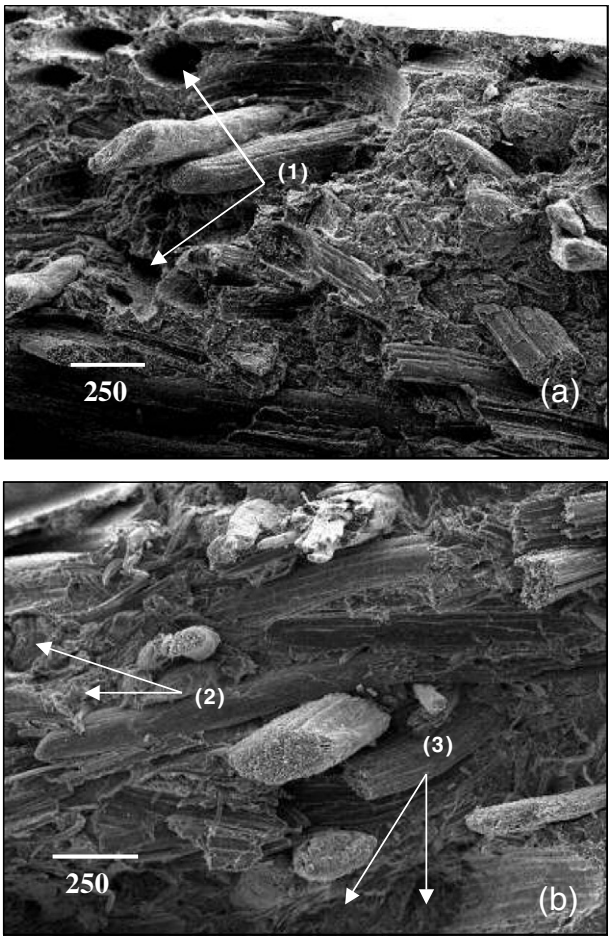

Fig. 9. Micrographs of scanning electron microscopy of fiber/HDPE composites (50 wt of fiber) using (a) unmodified or (b) modified blue agave fiber. In micrograph (a) arrows 1 indicate cavities where fibers were imbibed before impact assay; whereas in (b) arrows 2 and 3 indicate fraction of fibers that remained in the matrix after impact assay.

cavities. Likewise, some fibers with evidence of fracture remained on the matrix after the impact. Both features suggest good interfacial interaction between the modified fiber and the matrix, which was attributed to the fiber polarity reduction, product of esterification.

3.7. Rheological measurements

Figs. 10–12 present viscosity curves for unfilled polyethylene, unmodified and modified composites, respectively. The whole curves have been formed by the employment of the Cox–Merz rule (Bird, Armstrong, & Hassager, 1987). This rule establishes that $\eta = \eta^*$ when $d\gamma/dt = \omega$. Where η is the shear viscosity, η^* is the complex viscosity, $d\gamma/dt$ is the shear rate and ω is the oscillation frequency. The Cox–Merz rule has been suggested as a way of obtaining an improved relationship between the linear viscoelastic properties and the viscosity, expanding the viscosity curve toward high shear rates, in the power law region.

It is well known that at high shear rates, the angular velocity of rotational systems causes the displacement of

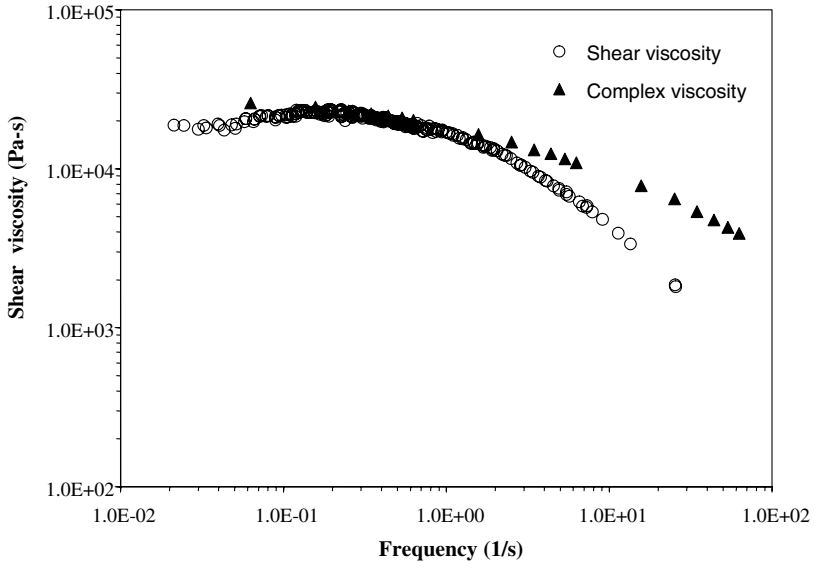

Fig. 10. Superimposed η and $\eta*$ curves for polyethylene according to Cox-Merz rule.

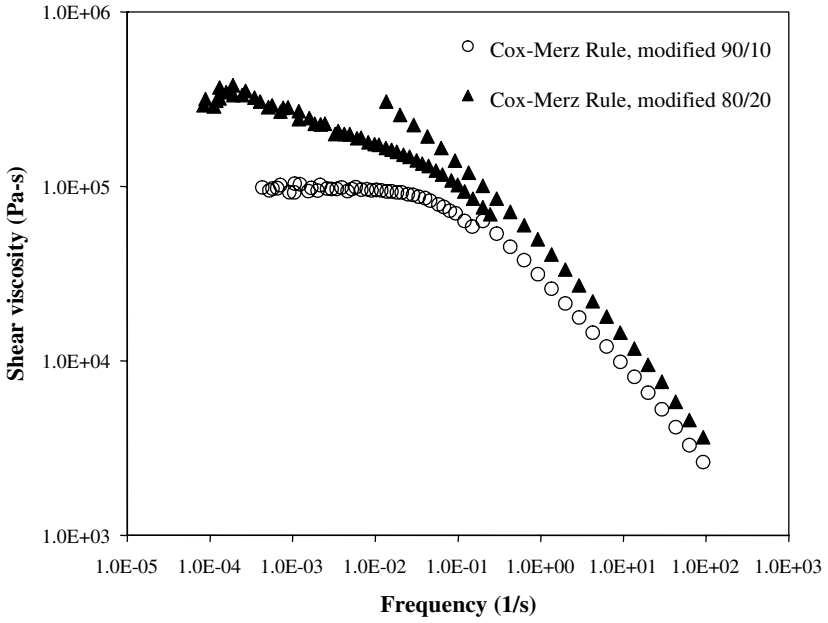

Fig. 11. Shear viscosity according to Cox–Merz rule for modified samples.

the fiber towards the perimeter of cone and plate or parallel plates devices. Similarly, in capillary rheometry the fiber tends to agglomerate in the center of the extruded filament, especially at high shear rates. In fact, attempts to obtain useful rheological parameters to fiber composite from torque rheometers have been done before (Ayora, Ríos, Quijano, & Márquez, 1997).

Fig. 10 presents the application of the Cox–Merz rule to unfilled polyethylene. It can be seen that in the low rate region a very good fit is attained for complex and shear viscosity, as frequently reported for the use of the Cox–Merz rule. However, literature also points out that in the power law region of the viscosity curve, significant deviations from the rule are observed (Bird et al., 1987), just as evidenced in this figure. Unlike the results for the polymeric matrix alone, in Fig. 11, is observed that the superposition of η and η* fits far well in the region of the power law for samples with modified fiber at weight concentrations of 10 and 20% (w/w), thus, allowing to obtain data in this important region of the curve. In the other hand, in Fig. 12, unmodified samples show a significant decoupling of the curves for rotational and oscillatory viscosity measurements, for both formulations, 90/10 and 80/20.

Strong differences in adjustment of η and η* trough Cox–Merz rule for modified and unmodified composites suggest that compatibilization process, indeed, influenced the interaction matrix–wood fiber which seems to play a

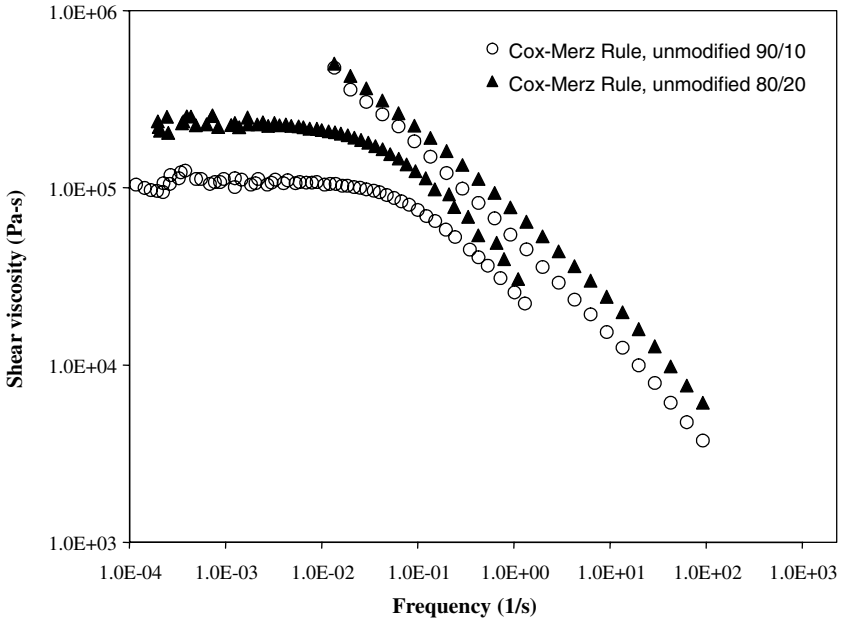

Fig. 12. Shear viscosity according to Cox–Merz rule for unmodified samples.

major role in the alignment and orientation patterns of the system.

4. Conclusion

It was shown that blue agave fiber can be successfully esterified by using a non-symmetric anhydride in non-aqueous media, which was confirmed by spectroscopic techniques which indicated the formation of C=O groups. It was found, however, that esterification efficiency depended strongly on anhydride accessibility towards the rich cellulose regions. Modified fiber hydrophobic nature was evident, since in an oil and water mixture the fiber preferred the former. Modification effect on fiber/HDPE composites was mainly observed on impact resistance properties, as modified composites showed a better performance than unmodified ones in all evaluated compositions. Finally, different adjustments of η and η^* to the Cox–Merz rule for modified and unmodified composites evidenced the effect of compatibilization in the flow properties.

Acknowledgements

Authors thank Antoine Gaset, Elisabeth Borredon, Ann Gschaedler, Enrique Torres, Manuel Roman, Daniel Lardizabal for their helpful assistance during this research.

References

Atalla, R. H., Gast, J. C., Sindorf, D. W., Bartuska, V. J., & Maciel, G. E. (1980). ^{13}C NMR spectra of cellulose polyphorms. *Journal of American Chemical Society, 102*, 3249–3251.

Ayora, M., Ríos, R., Quijano, J., & Márquez, A. (1997). Evaluation by torque-rheometer of suspensions of semi-rigid and flexible natural fibers in a matrix of poly(vinyl chloride). *Polymer Composites, 18*, 549–559.

Balasuriya, P. W., Ye, L., Mai, Y. W., & Wu, J. (2002). Mechanical properties of wood flake–polyethylene composites. II. Interface modification. *Journal of Applied Polymer Science, 83*, 2505–2521.

Bird, R. B., Armstrong, R. C., & Hassager, O. (1987) (2nd ed.). *Dynamics of polymeric liquids* (Vol. 1). New York: Wiley.

Bledzki, K., & Gassan, J. (1999). Composites reinforced with cellulose based fiber. *Progress in Polymer Science, 24*, 221–274.

Coutinho, F. M. B., Costa, T. H. S., & Carvalho, D. L. (1997). Polypropylene–wood fiber composites: Effect of treatment and mixing conditions on mechanical properties. *Journal of Applied Polymer Science, 65*, 1227–1235.

Coutinho, F. B., Costa, T. H. S., Carvalho, D. L., Gorelova, M. M., & Claudio de Santa Maria, L. (1998). Thermal behaviour of modified wood fibers. *Polymer Testing, 17*, 299–310.

Czimczik, C. I., Preston, C. M., Schmidt, M. W. I., Werner, R. A., & Schulze, E. D. (2002). Effect of charing mass, organic carbon, and stable carbon isotope composition of wood. *Organic Geochemistry, 33*, 1207–1223.

Chuavelon, G., Saulnier, L., Buleon, A., Thibault, J.-F., Gourson, C., & Benhaddou, R. (1999). Acid activation of cellulose and its esterification by long-chain fatty acid. *Journal of Applied Polymer Science, 74*, 1933–1940.

Ellis, W. D., & O'Dell, J. L. (1999). Wood–polymer composites made with acrylic monomers, isocianates, and maleic anhydride. *Journal of Applied Polymer Science, 73*, 2493–2505.

Girerdeau, S., Aburto, J., Vaca-Grcía, C., Alric, I., Borredon, E., & Gaset, A. (2001). An original method of esterification of cellulose and starch. In Chiellini et al. (Eds.), *Biorelated polymers: Sustainable polymer science and technology* (pp. 53). Dordrecht/Oxford: Klumer Academic/Plenum Publishers.

Ghosh, P., & Ganguly, P. K. (1994). Graft copolymerization of methyl methacrylate on jute using the aqueous IO^{4-}–Cu^{2+} combination as the initiator system and evaluation of the graft copolymer. *Polymer, 35*, 383–390.

Gupta, K. C., & Sahoo, S. (2001). Grafting of acrylonitrile and methyl methacrylate from their binary mixture on cellulose using ceric ions. *Journal of Applied Polymer Science, 79*, 767–778.

Gürdağ, G., Yaşar, M., & Gürkaynak, M. A. (1997). Graft copolymerization of acrylic acid on cellulose: Reaction kinetics of copolymerization. *Journal of Applied Polymer Science, 66*, 929–934.

Gürdağ, G., Güclü, G., & Özgümüş, S. (2001). Graft copolymerization of acrylic acid onto cellulose: Effects of pretreatments and crosslinking agent. *Journal of Applied Polymer Science, 80*, 2267–2272.

Hassan, M. L., Rowell, R. M., Fadl, N. A., Yacoub, S. F., & Christainsen, A. W. (2000). Thermoplasticization of bagasse. I. Preparation and characterization of esterified bagasse fiber. *Journal of Applied Polymer Science, 76*, 561–574.

Hassan, M. L., Rowell, R. M., Fadl, N. A., Yacoub, S. F., & Christainsen, A. W. (2000). Thermoplasticization of bagasse. II. Dimensional stability and mechanical properties of esterified bagasse composite. *Journal of Applied Polymer Science, 76*, 575–586.

Huang, Y., Zhao, B., Zheng, G., He, S., & Gao, J. (1992). Graft copolymerization of methyl methacrylate on stone ground wood using the H_2O_2–Fe^{2+} method. *Journal of Applied Polymer Science, 45*, 71–77.

Iñiguez-Covarrubias, G., Lange, S. E., & Rowell, R. M. (2001). Utilization of byproducts from the tequila industry. Part 1: Agave bagasse as a raw material for animal feeding and fiberboard production. *Bioresource Technology, 77*, 25–32.

Jandura, P., Kokta, B. V., & Riedl, B. (2000). Fibrous long-chain organic acid cellulose esters and their characterization by diffuse reflectance FT-IR spectroscopy, solid-state CP/MAS ^{13}C-NMR, and X ray diffraction. *Journal of Applied Polymer Science, 78*, 1354–1365.

Joseph, P. V., Rabello, M. S., Mattoso, L. H. C., Joseph, K., & Thomas, S. (2002). Environmental effects on the degradation behaviour of sisal fiber reinforced polypropylene composites. *Composites Science and Technology, 62*, 1357–1372.

Kim, U.-J., Kuga, S., Wada, M., Okano, T., & Kondo, T. (2000). Periodate oxidation of crystalline cellulose. *Biomacromolecules, 1*, 488–492.

Kontturi, E., Thüne, P. C., & Niemantsverdriet, J. E. (2003). Cellulose model surfaces-simplified preparation by spin coating and characterization by X-ray photoelectron spectroscopy, infrared spectroscopy, and atomic force microscopy. *Langmuir, 19*, 5735–5741.

Loría-Bastarrachea, M. I., Carrillo-Escalante, H. J., & Aguilar-Vega, M. J. (2002). Grafting of poly(acrylic acid) onto cellulosic microfibers and continuous cellulose filaments and characterization. *Journal of Applied Polymer Science, 83*, 386–393.

Matuana, L. M., Balatinecz, J. J., Sodhi, R. N. S., & Park, C. B. (2001). Surface characterization of esterified cellulosic fibers by XPS and FT-IR spectroscopy. *Wood Science and Technology, 35*, 191–201.

Mohanty, A. K., Mubarak, A. K., & Hinrichsen, G. (2000). Surface modification of jute and its influence on performance of biodegradable jute-fabric/biopol composites. *Composites Science and Technology, 60*, 1115–1124.

Nair, K. C. M., Thomas, S., & Groeninckx, G. (2001). Thermal and dynamic mechanical analysis of polystyrene composites reinforced with short sisal fibers. *Composites Science and Technology, 61*, 2519–2529.

Nielsen, L. E., & Landel, R. F. (1994). In *Mechanical properties of polymers and composites* (2nd ed.). New York: Marcel Dekker.

Rahman, L., Silong, S., Zin, W. M. D., Rahman, M. Z. A. B., Ahmad, M., & Haron, J. (2000). Graft copolymerization of methyl methacrylate onto sago starch using ceric ammonium nitrate as an initiator. *Journal of Applied Polymer Science, 76*, 516–523.

Rana, A. K., Mandal, A., & Banerjee, A. N. (2000). Jute sliver–LDPE composites: Effect of aqueous consolidation on mechanical and dynamic properties. *Journal of Applied Polymer Science, 76*, 684–689.

Ray, D., Sarkar, B. K., Das, S., & Rana, A. K. (2002). Dynamic mechanical and thermal analysis of vinylester–resin–matrix composites reinforced and alkali-treated jute fibers. *Composites Science and Technology, 62*, 911–917.

Redondo, S. U. A., Radovanovic, E., Goncalves, M. C., & Yoshida, I. V. P. (2002). Eucaliptus kraft pulp fibers as an alternative reinforcement of silicon composites. I. Characterization and chemical modification of eucaliptus fibers with organosilane coupling agent. *Journal of Applied Polymer Science, 85*, 2573–2579.

Román-Aguirre, M., Márquez-Lucero, A., & Zaragoza-Contreras, E. A. (2004). Elucidating the graft copolymerization of methyl methacrylate onto wood–fiber. *Carbohydrate Polymers, 55*, 201–210.

Rong, M. Z., Zhang, M.-Z., Liu, Y., Yang, G. C., & Zeng, H. M. (2001). The effect of fiber treatment on the mechanical properties of unidirectional sisal-reinforced epoxy composites. *Composites Science and Technology, 61*, 1437–1447.

Rowell, R. M., Simonson, R., Hess, S., Plackett, D. V., Cronshaw, D., & Dunningham, E. (1994). Acetyl distribution in acetylated whole wood and reactivity of isolated wood cell-wall components to acetic anhydride. *Wood Fiber Science, 26*, 11–18.

Simonsen, J., Jacobsen, R., & Rowell, R. (1998). Wood–fiber reinforcement of polystyrene–maleic anhydride copolymers. *Journal of Applied Polymer Science, 68*, 1567–1573.

Sun, R. C., Fan, g J. M., Tomkinson, J., Geng, Z. C., & Liu, J. C. (2001). Fractional isolation, physico-chemical characterization and homogeneous esterification of hemicelluloses from fast-growing poplar wood. *Carbohydrate Polymers, 44*, 29–39.

Sun, X.-F., Sun, R.-C., & Sun, J.-X. (2002). Acetylation of rice straw with or without catalyst and its characterization as a natural sorbent in oil spirit cleanup. *Journal of Agriculture and Food Chemistry, 50*, 6428–6433.

Thiebaud, S., & Borredon, M. E. (1995). Solvent-free wood esterification with fatty acid chlorides. *Bioresource Technology, 52*, 169–173.

Thiebaud, S., Borredon, M. E., Baziard, G., & Senocq, F. (1997). Properties of wood esterified by fatty-acid chlorides. *Bioresource Technology, 59*, 103–107.

Vaca-García, C., Thiebaud, S., Borredon, M. E., & Gozzelino, G. (1998). Cellulose esterification with fatty acids and acetic anhydride in lithium chloride/*N*,*N*-dimethylacetamide medium. *Journal of American Oil Chemists Society, 75*, 315–319.

Vaca-García, C., & Borredon, M. E. (1999). Solvent-free fatty acylation of cellulose and lignocellulosic wastes. Part 2: Reactions with fatty acids. *Bioresource Technology, 70*, 135–142.

Vázquez, A., Domínguez, V. A., & Kenny, J. M. (1999). Bagasse fiber–polypropylene based composites. *Journal of Thermoplastic Composites Materials, 12*, 477–497.

Xu, B., Simonsen, J., & Rochefort, W. E. (2001). Creep resistance of wood-filled polystyrene/high-density polyethylene blends. *Journal of Applied Polymer Science, 79*, 418–425.